Journal of Theoretical and Computational Chemistry, Vol. 1, No. 1 (2002) 1–15

FURTHER GENERALIZATION AND NUMERICAL IMPLEMENTATION OF PSEUDO-TIME SCHRÖDINGER EQUATIONS FOR QUANTUM SCATTERING CALCULATIONS

VLADIMIR A. MANDELSHTAM*
Chemistry Department, University of California at Irvine, Irvine, CA 92697, USA
mandelsh@uci.edu

ARNOLD NEUMAIER
Institut für Mathematik, Universität Wien Strudlhofgasse 4, A-1090 Wien, Austria
Arnold.Neumaier@univie.ac.at

Received 11 April 2002
Accepted 10 May 2002

We review and further develop the recently introduced numerical approach [Phys. Rev. Lett. **86**, 5031, (2001)] for scattering calculations based on a so called *pseudo-time Schrödinger equation*, which is in turn a modification of the damped Chebyshev polynomial expansion scheme [J. Chem. Phys. **103**, 2903, (1995)]. The method utilizes a special energy-dependent form for the absorbing potential in the time-independent Schrödinger equation, in which the complex energy spectrum is mapped inside the unit disk $E_k \to u_k$, where u_k are the eigenvalues of some explicitly known sparse matrix U. Most importantly for the numerical implementation, all the physical eigenvalues u_k are the extreme eigenvalues of U (i.e. $|u_k| \approx 1$ for resonances and $|u_k| = 1$ for the bound states), which allows one to extract these eigenvalues very efficiently by *harmonic inversion* of a pseudo-time autocorrelation function $y(t) = \phi^{\mathrm{T}} U^t \phi$ using the *filter diagonalization method*. The computation of $y(t)$ up to time $t = 2T$ requires only T sparse real matrix-vector multiplications. We describe and compare different schemes, effectively corresponding to different choices of the energy-dependent absorbing potential, and test them numerically by calculating resonances of the HCO molecule. Our numerical tests suggest an optimal scheme that provide accurate estimates for most resonance states using a single autocorrelation function.

Keywords: Quantum scattering; absorbing potential; resonances; Chebyshev polynomial expansion; iterative diagonalization; harmonic inversion; filter diagonalization method.

1. Introduction

In this paper we present a detailed description and further generalization of the methodology developed in the preceding works[1–4,6] for the efficient numerical solution of the quantum scattering problem associated with the time-independent Schrödinger equation

$$(H\psi)(r) = E\psi(r)\,. \tag{1}$$

Equation (1) may possess *bound states* with real energies E and wavefunctions $\psi(r)$ exponentially localized in space, and *resonance states* (Siegert states[7]) having complex energies with $\mathrm{Im}\, E \leq 0$. The latter behave like bound states in some compact subset Ω of the configuration space, but eventually grow exponentially outside of Ω, due to the outgoing asymptotic boundary conditions.

The corresponding bound state problem is conceptually simple and very well understood. The numerical solution of (1) at dissociation energies is much more difficult as it requires the solution of a boundary

*Corresponding author.

value problem. One can avoid the latter by the use of a so-called *optical* (*or absorbing*) *potential* $W(r)$ with $\operatorname{Im} W(r) \leq 0$ (in the sense that $i(W - W^*)$ is positive semidefinite, where * denotes conjugate transposition), that vanishes for $r \in \Omega$ and smoothly grows outside Ω. Numerically, this has negligible effect on the scattering solutions $\psi(r)$ of

$$(H\psi)(r) = (E - W(r))\psi(r) \tag{2}$$

inside Ω, i.e. the physically relevant region, and damps them outside Ω.[8] In other words, the complex absorbing potential forces the resonance solutions to behave like bound states everywhere without significantly affecting the energies E. In this framework the physically relevant part of the system is, therefore, dissipative and satisfies (1) only for $r \in \Omega$. Moreover, a general multichannel scattering problem can be considered with a numerically convenient form of $W(r)$, independent of the choice of coordinate system. The price for these benefits is that the originally hermitian problem becomes non-hermitian; but it is generally still complex symmetric.

Although to satisfy $\operatorname{Im} E \leq 0$ one only needs $\operatorname{Im} W \leq 0$, traditionally one simply uses a negative imaginary potential $W = -i\Gamma$ and gets the nonhermitian eigenvalue problem $(H - i\Gamma)\psi = E\psi$. The latter is generally much easier to handle numerically than the boundary value problem (1). As we already saw in Refs. 1 and 6 energy-dependent choices $W = W_E(r)$ are particularly useful.

The introduction of the absorbing potential leads to the *damped Green's function*[9–11]

$$G_W(E) := (H - E + W_E)^{-1}\,. \tag{3}$$

We assume that under suitable conditions on $W_E(r)$, similarly to the traditional case $W = -i\Gamma$,[11] $G_W(E)$ converges for any real E (and also for $\operatorname{Im} E \geq 0$) weakly to the ordinary Green's function

$$G(E) = \lim_{\varepsilon \downarrow 0} (H - E - i\varepsilon)^{-1}\,.$$

Practically, one usually needs to evaluate only certain matrix elements $\phi^{\mathrm{T}} G(E)\psi$, the basic numerical objects of quantum physics, from which most other quantities of interest (scattering amplitudes, reaction rates, etc.) can be computed (see, e.g., Refs. 9, 10, 12 and 13). These matrix elements are usually well approximated by $\phi^{\mathrm{T}} G_W(E)\psi$ if both ϕ and ψ have support in Ω.

Unfortunately, for very large systems with high density of states one may encounter numerical difficulties when trying to diagonalize a large nonhermitian matrix $H' = H + W$ or solve the linear system $(E - H')\phi(E) = \psi$ at many values of E using general iterative techniques for nonhermitian matrices. For instance, the Krylov subspace algorithms, such as the Lanczos diagonalization procedure, usually converge well for the extreme eigenvalues of H', while numerical problems may occur for interior complex eigenvalues of H' in the dense spectral regions, requiring more sophisticated schemes. As such a new technique called PIST was recently introduced by Carrington and co-workers.[14] The PIST method is based on a very efficient preconditioning within a QMR-Lanczos framework for iterative diagonalization of large and sparse DVR Hamiltonians with complex absorbing potentials. It is also appropriate to mention the time-dependent approach based on solution of the time-dependent Schrödinger equation,

$$\phi(t) = e^{-itH'}\phi(0) \tag{4}$$

which is widely used because of its simplicity (see, e.g. Refs. 12, 15 and 16), and can also be viewed as a Krylov subspace method with Krylov vectors

$$\phi(t) = U^t\phi(0) \tag{5}$$

generated by the powers of the evolution operator $U = e^{-iH'}$. The bound state eigenvalues $\lambda_k = e^{-iE_k}$ of U appear at the unit circle; the resonance eigenvalues near the unit circle, $|\lambda_k| \sim 1$, and satisfy $|\lambda_k| \leq 1$. That is, for a general initial state $\phi(0)$ all the physically important states ψ_k significantly contribute to $\phi(t)$, because they all correspond to the *extreme eigenvalues* of U (for which the relative weights defined by $|\lambda_k|^t$ are significant). This makes $\phi(t)$ a convenient basis for performing the spectral analysis of H'. For example, one can generate a time-correlation function

$$C(t) := \psi^{\mathrm{T}}\phi(t)\,. \tag{6}$$

Because the *time signal* $C(t)$ satisfies the form

$$C(t) := \sum_{k=1}^{K} d_k \lambda_k^t \tag{7}$$

with the weights $d_k = \psi^{\mathrm{T}}\psi_k\psi_k^{\mathrm{T}}\phi$, one can use Fourier spectral analysis to extract the desired eigenvalues E_k. Furthermore, the recently developed *Filter Diagonalization Method* (FDM)[2,17] (see also Refs. 18 and 19 on other related superresolution methods of spectral analysis) to solve the *harmonic inversion problem* (7) with the unknowns $\{d_k, \lambda_k\}$ generally leads to an enormous resolution enhancement, thus significantly reducing the required propagation time, as well as the overall numerical work. At first glance the time-dependent framework seems nearly optimal as the time correlation functions can be generated at low cost by various iterative techniques, e.g. the split-operator method.[20] The difficulty, however, arises when both the density and the number of states are very high, in which case the time domain data $C(t)$ must be very accurate at very long times in order to provide the adequate conditions for, e.g. FDM. Unfortunately, this requirement is very hard to satisfy, as it is difficult to accurately evaluate the matrix exponential $e^{-itH'}$ for a non-hermitian operator H' at very large values of t.

Apparently, for a quantum system with a Hamiltonian operator that is not explicitly time-dependent, there is nothing special about the time-dependent Schrödinger equation, except that it provides a convenient framework for both thinking and devising various numerical techniques to solve the time-independent problem, for example, those based on processing the time correlation functions. As such we can consider alternative dynamical schemes having the convenient structure of Eqs. (5)–(7), albeit with a pseudo-evolution operator U, somehow related to the underlying Hamiltonian H, but whose action on a vector can be evaluated easily. To this end the analogy between the standard time evolution and the Chebyshev recursion,

$$\phi(t) = 2H\phi(t-1) - \phi(t-2) \tag{8}$$

with initial conditions $\phi(0) = \phi$, $\phi(1) = H\phi$, or, more generally, damped Chebyshev recursion,[1]

$$\phi(t) = 2DH\phi(t-1) - D^2\phi(t-2) \tag{9}$$

with initial conditions $\phi(0) = \phi$, $\phi(1) = DH\phi$ and damping operator D ($D(r) = 1$ inside Ω and $D(r) \leq 1$, outside), was noticed and explored previously.[2,21–23] In Ref. 6, it was shown explicitly that a variant of Eq. (9),

$$\phi(t) = 2DH\phi(t-1) - D\phi(t-2) \tag{10}$$

with initial conditions $\phi(0) = \phi$, $\phi(1) = 0$, can be written in the familiar form (5) with some effective evolution operator U. The corresponding *pseudo-time Schrödinger equation* allows one to reap all the benefits of the time-dependent methods without having to deal with the standard time-dependent Schrödinger equation (4) involving nonhermitian Hamiltonian; it only requires the evaluation of a single H-matrix-vector product per time step and avoids the use of complex arithmetic, even when the absorbing potential is implemented.

As is well known, a (physical time) autocorrelation function at time $2t$ can be computed by solving the time-dependent Schrödinger equation up to time t, since one can use

$$C(t) := \phi^{\mathrm{T}}U^{2t}\phi = (U^t\phi)^{\mathrm{T}}(U^t\phi)$$

assuming only the complex symmetry of the evolution operator U, which is always easy to achieve, both with absorbing potential or without. For the Chebyshev autocorrelation function

$$y(t) := \phi^{\mathrm{T}}\phi(t) \tag{11}$$

where the vectors $\phi(t)$ are generated by Eq. (8), a factor of two saving is also well known (see, e.g. the discussion in Ref. 2):

$$y(2t+p) = 2\phi(t)^{\mathrm{T}}\phi(t+p) - y(p)$$

with $p = 0$, 1. When the damped scheme (9) is implemented, this recipe does not provide the correct autocorrelation function as defined by Eq. (11). Nevertheless, it was tried by Li and Guo.[4] The resulting doubled sequence, when processed by FDM, gave approximately correct resonance energies and widths. In Ref. 6, starting with the recursion formula (10), we derived an exact doubling scheme for the corresponding autocorrelation function (11):

$$y(2t+p) = \phi(t)^{\mathrm{T}}\phi(t+p) - \phi(t+1)^{\mathrm{T}}D^{-1}\phi(t+1+p)$$

with $p = 0$, 1.

In Ref. 5 the two schemes of Refs. 4 and 6 were applied to calculate the resonances of HN_2 and DN_2 and it was concluded that they are comparable within the reported numerical accuracy.

Here we note that the damping operator D in Eq. (9), as well as in Eq. (10), effectively leads to an energy-dependent complex absorbing potential $W_E(r)$, which may have a small or large real part relative to its imaginary part, depending on the particular recursion formula and the energy E. Usually, having too large $\mathrm{Re}\, W_E(r)$ is not desirable. Unfortunately, within the two frameworks one has little control over this circumstance. In the present paper, we re-derive and extend the above results by using a more flexible form for the absorbing potential, which can be adapted easily. The resulting pseudo-time Schrödinger equation is shown to be very convenient for calculating various dynamical properties, such as resonance parameters or matrix elements of the Green's function. The latter is carried out by generating the pseudo-time cross-correlation functions followed by their inversion. A numerical example based on very accurate resonance calculations reconfirms the validity of the theory and compares different damping schemes, suggesting an optimal scheme, that leads to accurate results with minimal computational effort.

2. Quadratic Eigenvalue Problem from Nonlinear Spectral Mapping

From now on, we assume that the Hilbert space is discretized so that the states are vectors $\psi \in \mathbf{C}^K$ and H, W are real symmetric $K \times K$ matrices, W diagonal, as e.g. in the case of a discrete variable representation.[31]

Let $\langle A\rangle_\psi := \psi^* A\psi/\psi^*\psi$ define the expectation value of the operator A. The original Hamiltonian matrix has its spectrum between $\bar{H} - \Delta H$ and $\bar{H} + \Delta H$. The quantity ΔH is called the *spectral range* and is defined by the particular basis set used to represent the Hamiltonian. However, to simplify the following equations we assume without loss of generality that the Hamiltonian matrix is already shifted and scaled so that

$$|\langle H - D_0\rangle_\psi| \le 1 \tag{12}$$

for any state ψ, where the diagonal real symmetric operator D_0 will be specified later. (In places where the scale factor ΔH is relevant, it will be inserted explicitly.) Such a scaling is implemented routinely in the framework of the Chebyshev polynomial expansion. We note that this typically moves the ground state energy to the lower edge of the spectrum, $E = -1$, while the energies of interest, including the dissociation energies, appear at the bottom of the spectrum, $E \sim -1$, as the total spectral range is usually an order of magnitude larger than the physically relevant spectral range.

We consider the choice

$$E - W = D_0 + \frac{1}{2}\, uD_1 + \frac{1}{2}\, u^{-1} D_2 \tag{13}$$

for some complex parameter u and real matrices D_0, D_1 and D_2, diagonal in the coordinate representation and satisfying

$$D_0(r) = 0, D_1(r) = 1, D_2(r) = 1 \quad \text{for } r \in \Omega\,. \tag{14}$$

This is a generalization of the previous results where the special cases using $D_0 = 0$, $D_2 = D_1^{-1}$ (as in Ref. 1) and $D_0 = 0$, $D_2 = 1$ (as in Ref. 6) were encountered.

To match the original problem in Ω, where the absorbing potential $W(r)$ vanishes, $u = u_E$ and $E = E(u)$ must be related by

$$u_E = E + i\sqrt{1 - E^2}\,, \quad \text{or} \quad E(u) = \frac{1}{2}\, u + \frac{1}{2}\, u^{-1} \tag{15}$$

as shown in Fig. 1. The absorbing potential then becomes a function of energy E (or, equivalently, of

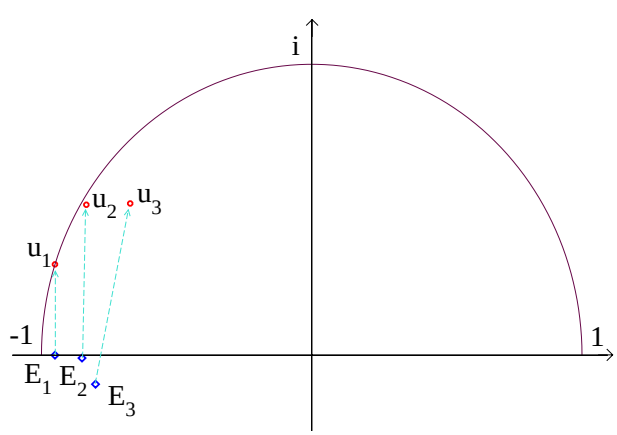

Fig. 1. The spectral mapping Eq. (15) maps a bound state E_1, which is real, to the upper half of the unit circle, and the resonance states, E_2 and E_3, with $\mathrm{Im}\, E_k < 0$, inside the upper half of the unit disk. $|u_2| \approx 1$ as it corresponds to a narrow resonance. (In practice the physically relevant states appear in a small low energy subset of the whole spectral domain.)

$u = u_E$):

$$W_E = \frac{1}{2}\,u(1 - D_1) + \frac{1}{2}\,u^{-1}(1 - D_2) - D_0\,. \qquad (16)$$

Insertion of (13) into (2) gives a nonlinear eigenvalue problem for u,

$$H\psi = \left(D_0 + \frac{1}{2}\,uD_1 + \frac{1}{2}\,u^{-1}D_2\right)\psi\,. \qquad (17)$$

We may think of this equation as an eigenvalue problem

$$H\psi = E(u)\psi \qquad (18)$$

involving an operator-valued u-dependent energy

$$E(u) = D_0 + \frac{1}{2}\,uD_1 + \frac{1}{2}\,u^{-1}D_2 \qquad (19)$$

that, by (14), reduces in Ω to the constant

$$E = \frac{1}{2}\,u + \frac{1}{2}\,u^{-1}\,.$$

3. Recasting to an Ordinary Eigenvalue Problem

Apparently, Eq. (17) is equivalent to a linear eigenvalue problem in a space of doubled dimension:

$$\hat{U}\hat{\psi} = u\hat{\psi} \qquad (20)$$

with 2K dimensional state vectors $\hat{\psi} = \begin{pmatrix}\psi\\ \psi'\end{pmatrix}$ and square $2K \times 2K$ matrix

$$\hat{U} := \begin{pmatrix} 0 & I \\ -D_1^{-1}D_2 & 2D_1^{-1}(H - D_0)\end{pmatrix} \qquad (21)$$

where I denotes the $K \times K$ unit matrix. This can be seen since (20) yields

$$\psi' = u\psi,\; D_1^{-1}D_2\psi - 2uD_1^{-1}(H - D_0)\psi + u^2\psi = 0\,.$$

Now multiplying by $D_1/2u$, we find (17).

We have rewritten the original nonhermitian eigenvalue problem (2) as another nonhermitian eigenvalue problem (20), but with the matrix $\hat{U}$ of doubled dimension. This would not necessarily be an advantage, if the eigenvalues of $\hat{U}$ did not possess the very important property that **the spectral domain of $\hat{U}$ is the unit disk**.

To see this, we consider an eigenpair (u, ψ) of (17) with $\psi^*\psi \neq 0$. Multiplying (17) by $2u\psi^*$ gives the quadratic equation

$$u^2\langle D_1\rangle_\psi - 2u\langle H - D_0\rangle_\psi + \langle D_2\rangle_\psi = 0$$

with solutions

$$u = \frac{\langle H - D_0\rangle_\psi \pm i\sqrt{\langle D_1\rangle_\psi\langle D_2\rangle_\psi - \langle H - D_0\rangle_\psi^2}}{\langle D_1\rangle_\psi}\,. \qquad (22)$$

To guarantee correct behavior in the following results, we need to apply the componentwise restrictions on the diagonal damping operators:

$$0 \le D_1^{-1} \le D_2 \le D_1 \ge 1 \qquad (23)$$

which together with the condition (12) imply that the square root is real. Thus, the solutions of (17) come in complex conjugate pairs, (u, ψ) and $(\bar{u}, \bar{\psi})$. The physically relevant eigenenergies with $\mathrm{Im}\,E \le 0$ come from u with $\mathrm{Im}\,u \ge 0$. Equation (22) implies that

$$|u|^2 = \frac{\langle H - D_0\rangle_\psi^2 + \langle D_1\rangle_\psi\langle D_2\rangle_\psi - \langle H - D_0\rangle_\psi^2}{\langle D_1\rangle_\psi^2}$$

$$= \frac{\langle D_2\rangle_\psi}{\langle D_1\rangle_\psi} \le 1 \qquad (24)$$

by Eq. (23). Thus, u is a complex number lying in the upper half of the unit disk (see Fig. 1). Moreover, $|u| = 1$ if and only if $\langle W\rangle_\psi = 0$, i.e. if and only if ψ has support in Ω, which is the case for the bound states. The states with $|u| \sim 1$ correspond to the narrow resonances.

The eigenpairs (u_k, ψ_k) of Eq. (17) can be used to evaluate the physically interesting quantities (e.g. the complex resonance energies E_k, scattering amplitudes, etc.). However, because of the nonlinearity they have somewhat different properties from those of the regular nonhermitian eigenvalue problem, which we now proceed to derive.

4. Completeness

As was already established, the eigenpairs $(u_k, \hat{\psi}_k)$ of $\hat{U}$ satisfy

$$\hat{\psi}_k = \begin{pmatrix}\psi_k\\ u_k\psi_k\end{pmatrix} \qquad (25)$$

where (u_k, ψ_k) is an eigenpair of (17). Since conversely, any such eigenpair determines an eigenpair of $\hat{U}$, the nonlinear eigenvalue problem (17) has at most $2K$ distinct eigenvalues. If there are $2K$ distinct eigenvalues $u_1, \ldots, u_{2K}$, the matrix $\hat{U}$ is diagonalizable, and there is a basis $\hat{\psi}_1, \ldots, \hat{\psi}_{2K}$ of eigenvectors of the form (25). Therefore, we can obtain the *completeness relations*, i.e. for any vector $\hat{\phi}$ we may write

$$\hat{\phi} := \begin{pmatrix} \phi_0 \\ \phi_1 \end{pmatrix} = \sum_{k=1}^{2K} \theta_k \hat{\psi}_k = \begin{pmatrix} \sum \theta_k \psi_k \\ \sum \theta_k u_k \psi_k \end{pmatrix} \tag{26}$$

with uniquely determined coefficients θ_k.

5. Orthogonality

Using (17), the symmetry of D_0, D_1, D_2 and H, and the fact that D_1 commutes with D_2, we may compute $\psi_j^{\mathrm{T}} H \psi_k$ in two different ways:

$$\begin{aligned} \psi_j^{\mathrm{T}} H \psi_k &= \psi_j^{\mathrm{T}} \left(D_0 + \frac{1}{2} u_k D_1 + \frac{1}{2} u_k^{-1} D_2 \right) \psi_k \\ &= \left(H \psi_j \right)^{\mathrm{T}} \psi_k \\ &= \psi_j^{\mathrm{T}} \left(D_0 + \frac{1}{2} u_j D_1 + \frac{1}{2} u_j^{-1} D_2 \right) \psi_k \,. \end{aligned}$$

For $j \neq k$, assuming that the eigenvalues are not degenerate, we may take the difference, multiply by the factor $2u_j u_k/(u_k - u_j)$, and find that the eigenfunctions satisfy the *orthogonality relations*

$$\psi_j^{\mathrm{T}} \left(D_2 - u_j u_k D_1 \right) \psi_k = 0 \,. \tag{27}$$

Provided that the left hand side of Eq. (27) does not vanish for $j = k$, we may normalize the eigenvectors so that

$$\psi_j^{\mathrm{T}} \left(D_2 - u_j u_k D_1 \right) \psi_k = \delta_{jk} \,. \tag{28}$$

Due to Eq. (25), the orthogonality relations can be rewritten in the double-dimension form:

$$\hat{\psi}_j^{\mathrm{T}} \hat{D} \hat{\psi}_k = \delta_{jk} \quad \text{with} \quad \hat{D} := \begin{pmatrix} D_2 & 0 \\ 0 & -D_1 \end{pmatrix} . \tag{29}$$

Using (29) and (26), we find:

$$\theta_k = \sum_j \theta_j \delta_{jk} = \sum_j \theta_j \hat{\psi}_j^{\mathrm{T}} \hat{D} \hat{\psi}_k = \hat{\phi}^{\mathrm{T}} \hat{D} \hat{\psi}_k \,. \tag{30}$$

6. Resolution of Identity

The orthogonality relations (29) and completeness imply the *resolution of identity*,

$$\hat{I} = \sum_{k=1}^{2K} \hat{\psi}_k \hat{\psi}_k^{\mathrm{T}} \hat{D} = \hat{D} \sum_{k=1}^{2K} \hat{\psi}_k \hat{\psi}_k^{\mathrm{T}} \tag{31}$$

which in the explicit form reads

$$\begin{aligned} \sum_{k=1}^{2K} \psi_k \psi_k^{\mathrm{T}} &= D_2^{-1} \\ \sum_{k=1}^{2K} u_k \psi_k \psi_k^{\mathrm{T}} &= 0 \\ \sum_{k=1}^{2K} u_k^2 \psi_k \psi_k^{\mathrm{T}} &= -D_1^{-1} \,. \end{aligned} \tag{32}$$

7. The Green's Function

For $u_E = E + i\sqrt{1 - E^2}$ and an eigenpair (u_k, ψ_k) of (17), we can write

$$(H - E + W_E)\psi_k = \frac{u_E - u_k}{2u_k u_E} \left(D_2 - u_k u_E D_1 \right) \psi_k \,.$$

Now multiplying from the right by $\frac{2u_k u_E}{u_E - u_k} \psi_k^{\mathrm{T}}$, summing over k and using the relations (32), we obtain

$$\begin{aligned} (E - H - W_E) \sum_{k=1}^{2K} \frac{2u_k u_E}{u_E - u_k} \psi_k \psi_k^{\mathrm{T}} \\ = \sum_{k=1}^{2K} (D_2 - u_k u_E D_1) \psi_k \psi_k^{\mathrm{T}} = I \,. \end{aligned}$$

This leads to a spectral representation of the damped Green's function $G_W(E) := (E - H - W_E)^{-1}$

$$G_W(E) = \sum_{k=1}^{2K} \frac{2u_k u_E}{u_E - u_k} \psi_k \psi_k^{\mathrm{T}} \,. \tag{33}$$

This expression uses the eigenvectors, which may be difficult to generate in large-scale computations. However, we shall see that Eq. (33) leads to iterative schemes for computing matrix elements of $G_W(E)$.

To derive these, we introduce the double-dimension Green's function

$$\hat{G}_W(E) := \sum_{k=1}^{2K} \frac{2u_k u_E}{u_E - u_k} \hat{\psi}_k \hat{\psi}_k^{\mathrm{T}} = \begin{pmatrix} G_W(E) & * \\ * & * \end{pmatrix} \tag{34}$$

whose top left corner suffices to represent the matrix element of the Green's function. Indeed, for suitable initial states ϕ_β and final states ϕ_α, we have

$$\phi_\alpha^{\mathrm{T}} G_W(E) \phi_\beta = \hat{\phi}_\alpha^{\mathrm{T}} \hat{G}_W(E) \hat{\phi}_\beta \tag{35}$$

with

$$\hat{\phi}_\beta := \begin{pmatrix} \phi_\beta \\ 0 \end{pmatrix}, \quad \hat{\phi}_\alpha := \begin{pmatrix} \phi_\alpha \\ 0 \end{pmatrix}. \tag{36}$$

$\hat{G}_W(E)$ is representable in terms of $\hat{U}$ as

$$\hat{G}_W(E) = 2(1 - \hat{U}/u_E)^{-1} \hat{U} \hat{D}^{-1} \tag{37}$$

which can be verified by applying Eqs. (34) and (37) to $\hat{D}\hat{\psi}_k$. (Note that the term $\hat{D}^{-1}$ in (37) is unnecessary as one usually considers initial states with support in Ω, where $\hat{D}_2 A = 1$, but we still prefer to keep it for completeness.)

8. The Pseudo-Time Schrödinger Equation

By replacing $(1 - \hat{U}/u_E)^{-1}$ in (37) with the geometric series we can express $\hat{G}_W(E)$ as a power series in $\hat{U}$:

$$\hat{G}_W(E) = 2 \sum_{t=1}^{\infty} u_E^{1-t} \hat{U}^t \hat{D}^{-1}. \tag{38}$$

This form using a discrete Fourier transform of the pseudo-evolution operator $\hat{U}^t$ is reminiscent of the integral Fourier transform of the true evolution operator

$$G(E) = i \int_0^\infty e^{-iHt} e^{iEt} dt.$$

However, for a given absorbing potential and basis set, e^{-iHt} can only be represented approximately, while Eq. (38) is *exact* as there is no approximation involved in evaluating $\hat{U}^t$. Because $\hat{U}$ is bounded inside the unit disk [cf. Eq. (24)], the expansion (38) also leads to a numerically stable procedure to compute the Green's function matrix elements

$$\phi_\alpha^{\mathrm{T}} G_W(E) \phi_\beta = 2 \sum_{t=1}^{\infty} u_E^{1-t} y_{\alpha\beta}(t) \tag{39}$$

where we have introduced the *pseudo-time correlation function*

$$\begin{aligned} y_{\alpha\beta}(t) &:= \hat{\phi}_\alpha^{\mathrm{T}} \hat{\phi}_\beta(t) \\ &= \hat{\phi}_\alpha^{\mathrm{T}} \hat{U}^t \hat{D}^{-1} \hat{\phi}_\beta \quad (t = 0, 1, \ldots). \end{aligned} \tag{40}$$

Equations (39) and (40) constitute an important result as they provide a convenient and efficient numerical framework based on solving the *pseudo-time Schrödinger equation*

$$\hat{\phi}_\beta(t) = \hat{U}^t \hat{D}^{-1} \hat{\phi}_\beta \quad (t = 0, 1, \ldots). \tag{41}$$

At each time step the vector $\hat{\phi}_\beta(t)$ can be used to form $y_{\alpha\beta}(t)$ by evaluating the scalar products with the $\hat{\phi}_\alpha$ states. The matrix elements of the Green's function can then be computed by Fourier spectral analysis of the corresponding pseudo-time correlation functions.

By noticing that the state vectors $\hat{\phi}_\beta(t)$ have the form

$$\hat{\phi}_\beta(t) := \begin{pmatrix} \phi_\beta(t) \\ \phi_\beta(t+1) \end{pmatrix} \quad \text{with} \quad \hat{\phi}_\beta(0) = \hat{D}^{-1} \begin{pmatrix} \phi_\beta \\ 0 \end{pmatrix}$$

(41) can be rewritten as a variant of a damped Chebyshev recursion formula

$$\phi_\beta(t) = D_1^{-1} [2(H - D_0)\phi_\beta(t-1) - D_2 \phi_\beta(t-2)], \quad t = 2, 3, \ldots \tag{42}$$

with initial conditions $\phi_\beta(0) = D_2^{-1} \phi_\beta$ and $\phi_\beta(1) = 0$.

The numerical cost of implementing a single step in (42) is essentially equal to that of multiplication of a real symmetric $K \times K$ matrix H by a real vector, as the other matrices are diagonal.

9. Time Doubling

We note that $\hat{D}\hat{U}^t$ is a complex symmetric matrix,

$$(\hat{D}\hat{U}^t)^{\mathrm{T}} = (\hat{U}^t)^{\mathrm{T}} \hat{D} = \hat{D}\hat{U}^t$$

which follows from the spectral representation

$$\hat{U}^t = \sum_{k=1}^{2K} u_k^t \hat{\psi}_k \hat{\psi}_k^{\mathrm{T}} \hat{D} \tag{43}$$

or can be verified directly by the matrix multiplication. Thus, for any t and s we can write

$$\begin{aligned} y_{\alpha\beta}(t+s) &= \hat{\phi}_\alpha^{\mathrm{T}} \hat{U}^{t+s} \hat{D}^{-1} \hat{\phi}_\beta \\ &= \hat{\phi}_\alpha^{\mathrm{T}} \hat{D}^{-1} \hat{D} \hat{U}^s \hat{U}^t \hat{D}^{-1} \hat{\phi}_\beta \\ &= [\hat{U}^s \hat{D}^{-1} \hat{\phi}_\alpha]^{\mathrm{T}} \hat{D} \hat{U}^t \hat{D}^{-1} \hat{\phi}_\beta \\ &= \hat{\phi}_\alpha^{\mathrm{T}}(s) \hat{D} \hat{\phi}_\beta(t) \end{aligned} \tag{44}$$

where $\hat{\phi}_\alpha(s)$ and $\hat{\phi}_\beta(t)$ are the solutions of Eq. (41) with initial conditions $\hat{\phi}_\alpha(0) = \hat{D}^{-1}\hat{\phi}_\alpha$ and $\hat{\phi}_\beta(0) = \hat{D}^{-1}\hat{\phi}_\beta$. This means that $y_{\alpha\beta}(t)$ can be computed up to time $2T$ using

$$y_{\alpha\beta}(2t+p) = \hat{\phi}_\alpha(t)^{\mathrm{T}} \hat{D} \hat{\phi}_\beta(t+p)\,, \quad p = 0, 1 \tag{45}$$

concurrently with the computation of $\hat{\phi}_\alpha(t)$ and $\hat{\phi}_\beta(t)$ for $t = 0, \ldots, T$. In particular, the calculation of an autocorrelation function $y_{\alpha\alpha}(t)$ up to time $2T$ requires $\sim T$ multiplications of the real and sparse $K \times K$ H-matrix on a vector with just a few vectors stored at a time.

10. Resonance Calculation by Harmonic Inversion of Pseudo-Time Correlation Functions

The spectral mapping $E_k \to u_k$ (15) moves all the physically relevant eigenvalues to the vicinity of the unit circle, i.e. they all become extreme (or nearly extreme for the resonances) eigenvalues of $\hat{U}$. This, in turn, creates very favorable conditions for computing these eigenvalues iteratively using any suitable Krylov subspace method with the Krylov vectors generated by the powers of $\hat{U}$, because the extreme eigenstates contribute mostly to the latter. In the present framework, such a strategy of computing the bound and resonance state energies, in its most simple and convenient form, boils down to the *harmonic inversion* of pseudo-time correlation functions (40), which due to Eq. (43) satisfy

$$y_{\alpha\beta}(t) = \sum_{k=1}^{2K} d_{\alpha\beta k} u_k^t \tag{46}$$

with

$$d_{\alpha\beta k} = b_{\alpha k} b_{\beta k} = (\hat{\phi}_\alpha^{\mathrm{T}} \hat{\psi}_k)(\hat{\psi}_k^{\mathrm{T}} \hat{\phi}_\beta)\,.$$

(Note that the resolution of identity (31) implies $\hat{\phi}_\alpha = \hat{D} \sum_k \hat{\psi}_k \hat{\psi}_k^{\mathrm{T}} \hat{\phi}_\alpha = \hat{D} \sum_k b_{\alpha k} \hat{\psi}_k$.)

Thus the nonlinear eigenvalue problem (17) is reduced to the signal processing problem of finding the spectral parameters $(u_k, d_{\alpha\beta k})\,(k = 1, \ldots, 2K)$ satisfying Eq. (46) for the sequence(s) $y_{\alpha\beta}(t)$ computed by Eqs. (42) and (40). The simplest procedure then corresponds to considering a single doubled autocorrelation function $y_{\alpha\alpha}(t)$ with $t = 0, \ldots, 2T$. In exact arithmetic the harmonic inversion of such a sequence will give the exact results if $T > 2K$, thus, using only $T \sim 2K$ of real matrix-vector products. However, this is impractical as it would formally require one to solve a $T \times T$ eigenvalue problem. To reduce the computational burden and to maintain numerical stability the eigenvalues are extracted very efficiently in a small Fourier subspace by the FDM.[2,17] If we introduce the unscaled energy $\varepsilon = E\Delta H + \bar{H}$, the required length $2T$ of the doubled sequence needed to converge an eigenenergy E_k [cf. Eq. (15)] by the FDM will be defined by the locally averaged density of states $\rho(\varepsilon)$ for $E_k \sim E$ and the spectral range ΔH of the Hamiltonian matrix according to the approximate relationship[2,32]

$$T \geq 2\pi \Delta H \rho(\varepsilon) \sqrt{1 - E^2} \tag{47}$$

where the factor $\sqrt{1-E^2}$ arises from the $u \to E$ mapping (15).

Because the eigenpairs come in complex conjugate pairs (u_k, ψ_k) and $(\bar{u}_k, \bar{\psi}_k)$, once the initial vectors $\hat{\phi}_\alpha$ and $\hat{\phi}_\beta$ are real (46) becomes

$$y_{\alpha\beta}(t) = \mathrm{Re} \sum_{k=1}^{K} d_{\alpha\beta k} u_k^t \tag{48}$$

where only the physical eigenvalues with $\mathrm{Im}\, u_k > 0$ are included in the sum. Note also that for the pure bound state problem, when $|u_k| = 1$ and the eigenfunctions ψ_k (and, therefore, the coefficients $d_{\alpha\beta k}$) are real, the sequence $y_{\alpha\beta}(t)$ has the time reversal symmetry

$$y_{\alpha\beta}(-t) = \bar{y}_{\alpha\beta}(t) \tag{49}$$

which further doubles the total time by extending the signal to the negative times.

11. Inversion of the Time Cross-Correlation Functions

As was previously shown in Ref. 3 one can, in principle, compute matrix elements $\phi_\alpha^{\mathrm{T}} G_W(E) \phi_\beta$ for *any*

ϕ_α, ϕ_β by (i) propagating a *single* initial state ϕ_0 using Eq. (42), (ii) computing the cross-correlation functions $y_{00}(t)$, $y_{0\alpha}(t)$ and $y_{0\beta}(t)$ using Eq. (40) and (iii) solving the corresponding harmonic inversion problems (46) for the unknown parameters $\{u_k, b_{\alpha k}, b_{\beta k}\}$ to evaluate

$$\phi_\alpha^{\mathrm{T}} G_W(E)\phi_\beta = \sum_{k=1}^{2K} \frac{2u_k u_E}{u_E - u_k}\, b_{\alpha k} b_{\beta k}\,. \qquad (50)$$

Moreover, a more stable evaluation of the matrix element $\phi_\alpha^{\mathrm{T}} G_W(E)\phi_\beta$ may be achieved using the *Regularized Resolvent Transform* (RRT) which was described in detail in Ref. 18. The advantage of RRT is that the calculation of spectral parameters $\{u_k, b_{\alpha k}, b_{\beta k}\}$ is avoided, the spectra are computed directly by matrix inversion or by solving linear systems.

This results in an enormous numerical saving as, traditionally, the time-dependent approaches require multiple initial state propagations in order to compute, for example, the full S-matrix or cumulative reaction probability. However, the described approach, although formally exact (in exact arithmetic), is applicable only when the dynamics is governed solely by narrow resonances: the parameters of very broad resonances (or poles of the Green's function) are generally grossly inaccurate, leading to very unstable spectral estimation by Eq. (50). A significant numerical saving in cases with broad resonances is, however, achievable if one adapts another strategy in which one (i) propagates a set of initial states $\{\phi_\beta\}$, ($\beta = 1, \ldots, L$) using Eq. (42), (ii) computes the *cross-correlation matrix* using the doubling formula (45) and (iii) solves the harmonic inversion problem (46) for the $L \times L \times 2T$ data matrix (see Refs. 3, 17 and 18). As argued in Ref. 3, this approach has a potential of reducing the total propagation time T required for the accurate harmonic inversion by a factor of L, i.e. preserving the total number of matrix-vector multiplications, $N_{\mathrm{total}} = L \times T$. Unfortunately, to use the doubling trick (45) in this case, the storage requirement to generate the cross-correlation matrix is increased because of the need to simultaneously propagate L states rather than one.

12. Practical Considerations: Choosing the Absorbing Potential

The physical observables can generally be computed from the Green's function matrix elements at real energies. For this reason and for the sake of simplicity in the following analysis we will assume the energy E to be real. However, essentially the same conclusions hold for complex energies near the real axis, i.e. including the narrow resonances.

Since $u_E^{-1} = E - i\sqrt{1 - E^2}$, our construction (16) leads to the complex valued absorbing potential

$$W_E = E\left(1 - \frac{D_1 + D_2}{2}\right) - D_0 - i\sqrt{1 - E^2}\,\frac{D_1 - D_2}{2}\,. \qquad (51)$$

The restrictions (23) on the choice of D_1 and D_2, imply that $\mathrm{Im}\, W_E \le 0$. This is essential since it leads to the correct limit for the Green's function $G_W(E)$ on the real line. The real part $\mathrm{Re}\, W_E$ is generally nonzero; although its role is not crucial in scattering calculations, significant values of $\mathrm{Re}\, W_E$ may or may not be desirable. In particular, a positive $\mathrm{Re}\, W_E$ reduces the total density of states $\rho(E)$, while affecting only slightly the resonance states, and thus, it may accelerate the convergence [cf. Eq. (47)]. At the same time $\mathrm{Re}\, W_E$ may get excessively large compared to $\mathrm{Im}\, W_E$, for example, near the spectral edge, $E \sim -1$, if $D_0 = 0$. It is not absolutely clear without numerical tests how this artifact will affect the results, while it can be controlled if the matrix D_0, which is in principle unrestricted, is used. Namely, relatively to the total spectral range ΔH (which becomes unity after scaling of H), the physical energy range is generally only a small part of the unit disk. Therefore, within this range we can often assume $W_E \approx W_{E_0}$ for some reference energy E_0. Now by setting

$$D_0 = E_0\left(1 - \frac{D_1 + D_2}{2}\right), \qquad (52)$$

we can significantly reduce (or increase) the real component if needed,

$$\mathrm{Re}\, W_E = (E_0 - E)\left(\frac{D_1 + D_2}{2} - 1\right) \qquad (53)$$

without affecting $\mathrm{Im}\, W_E$. In order to avoid negative $\mathrm{Re}\, W_E$ in the physically relevant energy region, it suffices to take E_0 higher than the maximum energy of interest.

Clearly, the behavior of the absorbing potential W_E where it starts to turn on has the main effect for

the scattering calculations. In fact, as follows from our numerical tests, the best performance is achieved when both $D_1 \approx 1$ and $D_2 \approx 1$ over almost the entire grid used to represent the state vectors. Therefore, it is convenient to use the real operators γ_1 and γ_2 defined by

$$D_1 = e^{\gamma_1}\,, \quad D_2 = e^{-\gamma_2} \tag{54}$$

which vanish in Ω and slowly turn on in the absorbing region, and assume that both γ_1 and γ_2 are small. By expanding into the Taylor series up to the second order, we can rewrite (51) as

$$W_E \approx (E_0 - E)\left(\frac{\gamma_1 - \gamma_2}{2} + \frac{\gamma_1^2 + \gamma_2^2}{4}\right) - i\sqrt{1-E^2}\left(\frac{\gamma_1 + \gamma_2}{2} + \frac{\gamma_1^2 - \gamma_2^2}{4}\right). \tag{55}$$

We expect the results to be generally insensitive to a particular form of W_E as long as γ_1 and γ_2 are sufficiently smooth and have sufficiently large spatial extension. So here we only consider the two special choices.[1,6]

M&T scheme: $\gamma_1 \equiv \gamma_2 \equiv \gamma$ as in Ref 1 with $\gamma(R) > 0$:

$$W_E = (E_0 - E)(\cosh(\gamma) - 1) - i\sqrt{1-E^2}\sinh(\gamma)\,. \tag{56}$$

As follows from the expansion (55), $\operatorname{Re} W_E$ is already small as its leading term becomes quadratic in γ, while $\operatorname{Im} W_E$ is linear:

$$W_E \approx \frac{1}{2}(E_0 - E)\gamma^2 - i\sqrt{1-E^2}\,\gamma\,. \tag{57}$$

Note again that in the computations involving molecular vibrational spectra the energies of interest are usually close to the bottom of the spectral range of the scaled Hamiltonian matrix, $E \sim -1$. Defining the shifted energy $\varepsilon := E + 1$ with zero at the bottom of the spectrum and assuming $\varepsilon \ll 1$, we can approximately determine how the absorbing potential depends on energy:

$$W_E \approx \frac{1}{2}(\varepsilon_0 - \varepsilon)\gamma^2 - i\sqrt{2\varepsilon}\,\gamma\,. \tag{58}$$

A convenient choice for γ in Eq. (56) corresponds to $\gamma(R)$ being a function of the reaction coordinate R, vanishing in the interaction region, $R < R_\Omega$, and smoothly growing in the absorbing region, $R_\Omega < R < R_{\max}$, where $R_{\max}$ defines the fartherst grid point:

$$\gamma(R) = \frac{\lambda}{\sqrt{\Delta H}}\left(\frac{R - R_\Omega}{R_{\max} - R_\Omega}\right)^2. \tag{59}$$

Here λ is an adjusting parameter. As follows from Eq. (58), the factor $\sqrt{\Delta H}$ in Eq. (59) minimizes the sensitivity of $\operatorname{Im} W_E$ to the actual spectral range ΔH of the Hamiltonian matrix. Note that with this construction $\operatorname{Re} W_E$ will be sensitive to ΔH, but generally small.

N&M scheme: $\gamma_2 \equiv 0$ and $\gamma_1 \equiv 2\gamma$, as in Ref. 6:

$$W_E = \frac{E_0 - E - i\sqrt{1-E^2}}{2}\,(e^{2\gamma} - 1) \tag{60}$$

$$\approx (E_0 - E - i\sqrt{1-E^2}\,)\gamma \tag{61}$$

where we retained only the leading linear term. Further assuming ε to be small, we obtain

$$W_E \approx (\varepsilon_0 - \varepsilon)\gamma - i\sqrt{2\varepsilon}\,\gamma\,. \tag{62}$$

Thus the difference between M&T and N&M schemes is the different behavior of $\operatorname{Re} W_E$. This difference may be eliminated almost completely by manipulating with D_0. In the next section, we examine the effect of this difference on the quality of the resonance calculations.

In order to identify the true resonances and obtain the best resonance parameters estimates for given basis set, the common practice is to search for stationary eigenvalues E_k under variations of the absorbing potential.[8,11,26] This is usually done by varying its amplitude, which here corresponds to the free parameter λ. (One could possibly change instead E_0, or treat E_0 as a function of λ.) The eigenvalue trajectories $E_k(\lambda)$ are then analyzed for stationary points, such as the point of maximum curvature, which in an ideal case may be a cusp (see Fig. 2). One way to practically find such a point is to minimize the derivative $dE_k/d\lambda$. Some of the complex eigenvalues are extremely sensitive to λ. This sensitivity is practically used to reject the non-resonant eigenvalues. The generation of the eigenvalue trajectories usually significantly increases the computational time, while a reasonable accuracy for most states can be achieved from a single or a few runs using an *a priori* established optimal value

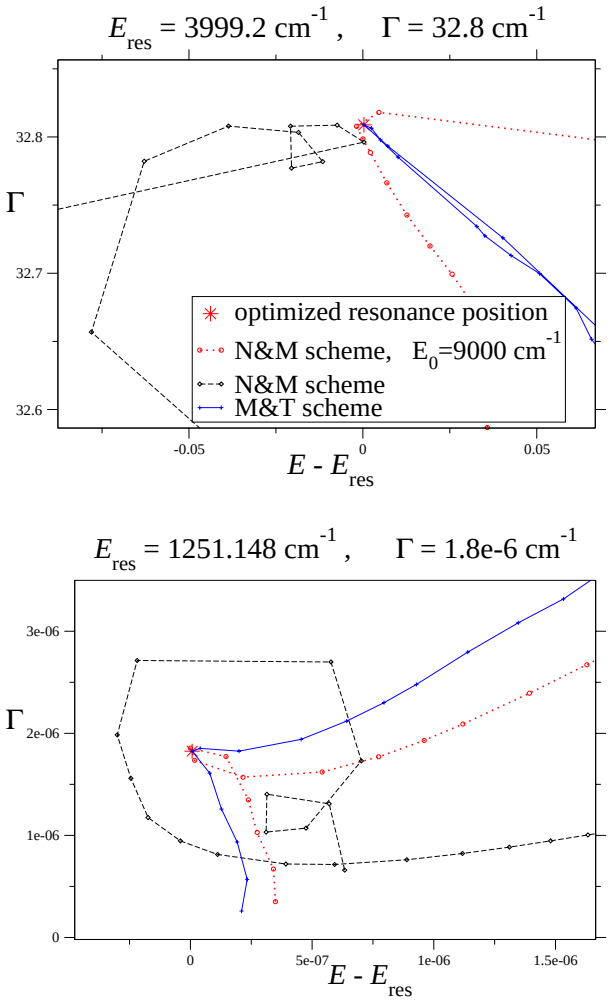

Fig. 2. Typical eigenvalue trajectories for two resonance states obtained using three different damping schemes (see text).

of λ. Therefore, such a search is justified only if a very high accuracy for all resonances is needed. The cases where eigenvalue trajectory analysis may be necessary include extremely narrow (shape) resonances. If the complex trajectories are not available, the decision whether a particular E_k is true resonance or not may be based on analysis of the weight $d_k = \left(\phi_0^{\mathrm{T}}\psi_k\right)^2$ which is very small for a non-resonant state if the initial state ϕ_0 is localized in the interaction region.

13. Numerical Example: Resonances of the HCO Molecule

In this section we apply the present approach using pseudo-time autocorrelation functions for an accurate computation of the nonrotating HCO resonances. This system has been used in the past by various groups as a benchmark problem to test new approaches (see the comprehensive review[27] and references therein). In particular, the first resonance calculation using FDM was applied to HCO.[28] We use the potential energy surface of Keller *et al.*[29] where a resonance calculation was also performed and the resonances were assigned. Recently, Poirier & Carrington[27] applied the above mentioned PIST method to reproduce these results but with a significantly higher accuracy and numerical efficiency. We use the latter results as a reference. Although, PIST is a very efficient alternative to the present technique, in our study we do not make an adequate comparison of the two methods as it would require the use of, at least, the same basis set.

The present choice of the basis is the most primitive direct-product Jacobi coordinate DVR grid, similar to that used in Ref. 28. The results reported below correspond to a particular choice of the grid and absorbing potential parameters, which, as was verified by comparison with calculations using different parameters, provided extremely accurate results for the resonances in the energy region below 9000 cm^{-1}. In order to avoid an extensive search for optimal basis set parameters, our strategy is to use a larger and denser grid than may be necessary to garantee high accuracy. This strategy is justified by a very favorable numerical scaling of the present technique with the basis size.

For $R_{\mathrm{H-CO}}$ (the dissociation coordinate) we used 160 sinc-DVR[24] points in the interval $[2, 8]$ a$_0$, contracted to $N_R = 40$ points by means of the HEG[25] method using the eigenfunctions of the 1D Hamiltonian defined by $V(R) = \min_{r,\theta} V(R_e, r, \theta)$, where $V(R_e, r, \theta)$ is the 3D potential of HCO in the Jacobi coocrdinates. For the r_{CO} coordinate we used 64 sinc-DVR points in the interval $[1.8, 3.5]$ a$_0$, contracted to $N_r = 16$ points. For the angular variable we used $N_\theta = 46$ Gauss-Legendre-quadrature DVR points. In order to reduce the Hamiltonian spectral range ΔH we replaced the high values of the potential by the cutoff value $V_{\mathrm{cut}} = 25{,}000$ cm^{-1}. This resulted in $\Delta H = 44{,}654$ cm^{-1}. We note, that for the present approach the quality of the grid basis is measured by ΔH, which directly affects the convergence [cf. Eq. (47)]. Since our basis is very primitive the spectral range is relatively high. One may argue

though that a primitive basis has the advantage of minimizing the number of adjusting parameters and leads to a fast matrix-vector multiplication for given grid size.

Here we report results corresponding to the three different schemes: (I) N&M scheme with D_0 defined by $E_0 = 9{,}000$ cm^{-1} (the maximum energy of interest), (II) N&M scheme with $D_0 = 0$, and (III) M&T scheme with $D_0 = 0$. (We note that the use of nonzero D_0 in the M&T scheme has almost no effect as $\mathrm{Re}\, W_E$ is already very small in this case.)

For each scheme the damping potential has been taken in the form (59) with $R_\Omega = 5$ a$_0$. For this study we varied the strength parameter λ in the range $[0.0002, 0.6]$ with a logarithmic distribution of 22 λ values.

For each λ an autocorrelation function $y(t)\,(t = 0, \ldots, 2T = 20{,}000)$ with a random initial vector was generated using $T = 10{,}000$ matrix-vector multiplications. Calculation of a single autocorrelation function takes 239 sec on an Athlon 1.8 GHz pc using the gnu g77 Fortran compiler. Because the latter is very inefficient, the reported timing only gives a rough estimate of the algorithm efficiency. The autocorrelation functions were then inverted by our quadruple-precision FDM code.[30] For a large enough value of λ, the FDM results converge for most resonance states using $T \approx 7{,}000$, however, to maintain an extremely high accuracy, especially for the lowest sharp resonance $|013)$ with width $\Gamma = 3 \cdot 10^{-8}$ cm^{-1} and for small λ values, we needed $T \approx 10{,}000$. (The effective density of states, that includes both the true resonance states and states representing the continuum, becomes high for small λ.) Of course, a smaller grid and lower V_{cut} would result in a smaller ΔH reducing the needed number of iterations accordingly. Also note that because only small generalized eigenvalue problems are encountered in FDM, the cpu-time increase due to the use of the quadruple precision is not essential, while it improves the accuracy and accelerates the convergence of the extracted eigenvalues significantly, compared to the double precision code. For the present "toy problem" the harmonic inversion part is as time-consuming (with quadruple precision) as the correlation function generation, however, the former becomes relatively negligible for bigger systems.

Let $E_{\mathrm{res}} := \mathrm{Re}\, E_k$ define the positions and $\Gamma_k := -2\,\mathrm{Im}\, E_k$, the widths of the resonances. The eigenvalue trajectories $E_k(\lambda)$ with $\Gamma_k < 120$ cm^{-1} are plotted in the complex plane and the most stationary point (see above) is assumed as the best resonance energy estimate. The eigenvalue trajectories showing no stationary points and/or not appearing in different schemes are rejected. In Fig. 2, we show the eigenvalue trajectories generated using the three different damping schemes decribed above for two states (a) with $E_{\mathrm{res}} = 3999.2$, $\Gamma = 32.8$ cm^{-1} and (b) $E_{\mathrm{res}} = 1251.148$, $\Gamma = 1.8 \cdot 10^{-6}$ cm^{-1}. Schemes I and III result in quite different trajectories for most λ values but have easily identified stationary points (cusps) for about the same value λ. These stationary points are very close to each other. At the same time, scheme II gives more complex trajectories that circle around the resonance position, but have no well identified stationary point. Similar patterns are observed for most other states. Note also, that for some resonances the cusps may not exist, however having the two types of trajectories helps one to better locate the complex resonance energy by taking the point where the trajectories of different types approach each other. Furthermore, scheme III generally results in sharpest cusps, but because it corresponds to a smaller $\mathrm{Re}\, W_E$, it also requires larger values of T for an accurate harmonic inversion, as smaller $\mathrm{Re}\, W_E$ corresponds to higher density of states. For the same reason, scheme II needs the smallest T.

Surprisingly, for most resonances, the stationary point in the eigenvalue trajectories are approached for the same value $\lambda_{\mathrm{opt}} = 0.08$, while only for a few extremely sharp resonances near the dissociation threshold $E_{\mathrm{dis}} = 1{,}086$ cm^{-1}, the values $E_k(\lambda = 0.08)$ give poor estimates of the true complex resonance energies. For these states the optimal λ is a monotonically growing function of $E_{\mathrm{res}} - E_{\mathrm{dis}}$; the optimal λ for the sharpest state, $|013)$, is $\lambda_{\mathrm{opt}} \approx 0.0016$ and for the next state, $|005)$, it is $\lambda_{\mathrm{opt}} \approx 0.0064$. The need to generate the eigenvalue trajectories significantly increases the overall computational cost. By setting $\lambda = 0.08$ with the present choice of $\gamma(R)$, one can use a single autocorrelation function to obtain good resonance estimates for most states, but a few. Of course, with a single autocorrelation function, one (i) cannot access extremely high accuracy for all the resonances and (ii) one loses the convenient tool to identify the true resonances.

There is no simple way to determine the error bounds other than by comparing the results using

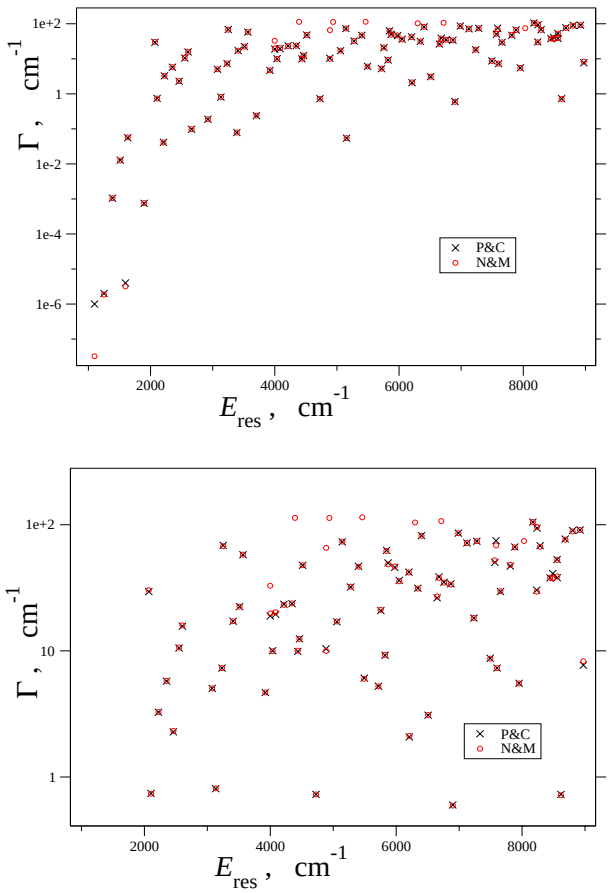

Fig. 3. The widths Γ versus resonance positions $E_{\rm res}$ shown for two different scales. The present results (circles) are obtained using scheme 1 (see text). The crosses are the results of Poirier & Carrington.[27]

different parameters. For this purpose we performed another set of calculations in which we used $N_R \times N_r \times N_\theta = 47 \times 18 \times 44$ with the absorbing region $R \in [5.5, 9.0]$ a_0 and the same set of the λ values. The energy and width differences between the two computed sets of resonances were then used to estimate the corresponding errors. (In addition, the adequacy of the estimates was checked by similar, additional computations.) The accuracy in the positions of the resonances varies and depends mostly on Γ_k. It also depends in a less systematic way on the quantum numbers. For narrow resonances ($\Gamma_k \sim 1$ cm^{-1} or less) the accuracy in the position is of the order of 0.01 cm^{-1} or better, while for the other states with $\Gamma_k < 100$ cm^{-1} it is generally of the order of 0.1 cm^{-1}. We believe that, for the given potential, generally the error in the reported widths is less than 1%, although this may not be true for some states. Thus the accuracy is usually higher than justified by the (additional) inaccuracies, such as uncertainties in the potential energy surface. For practical purposes a 10% accuracy for the widths is usually more than acceptable.

Figure 3 and Table 1 summarize our results obtained with scheme 1 and compare them with the calculation of Poirier & Carrington.[27] The assignments of the resonance states have been made by Keller *et al.* [29] The latter results for the resonance parameters are not displayed here as they are less accurate. The last digit in the "present results" is believed to be uncertain. This can serve as a rough error estimate; it was obtained by comparing the results with a second calculation using different DVR grid parameters and absorbing potential. However, one should be cautious to not overestimate the reliability of the reported accuracy, as no convergence tests, systematically varying all the computational parameters, were performed. Such an analysis is very costly. For the same reason, we would not be extremely surprised if more accurate calculations later reveal additional resonance states.

Our results generally agree very well with those of Poirier & Carrington, although some states are missing in the latter, such as the broad resonance shown in Fig. 2; this is likely due to a too generous rejection criterion used by Poirier & Carrington to identify the true resonances. Note also that for the first two sharp resonances, Poirier & Carrington did not report accurate width estimates. On the other hand, for the HCO molecule, PIST appeared very efficient (requiring relatively few matrix-vector multiplications to accurately compute the resonances) and relatively small cpu-time. However, under the present circumstances, a fair comparison between the present approach and PIST[27] is not possible; e.g. very different basis sets were used in the two cases.

To conclude, at least for the resonance calculations, the present approach appears very reliable, accurate and efficient. It requires a minimal number of adjusting parameters and scales favorably with the size of the system. The method is quite flexible in the choice of the damping scheme, but according to our tests an optimal choice corresponds to scheme I (see above) with $\lambda \approx 0.08$.

We make the corresponding Fortran codes available upon request (e-mail: mandelsh@uci.edu).

Table 1. Resonance energies $E_{\rm res}$ and widths Γ ($\rm cm^{-1}$) for the nonrotating HCO molecule. The quantum numbers describe, respectively, the CH stretch, the CO stretch, and the bend. The last digit in the "present results" is believed to be uncertain (see text), although an accurate error estimate is unknown.

Keller *et al.*[29]	Poirier and Carrington[27]		Present results		Ref. 29	Ref. 27		Present results	
State	$E_{\rm res}$	Γ	$E_{\rm res}$	Γ	State	$E_{\rm res}$	Γ	$E_{\rm res}$	Γ
|013)	1098.7934	≤1e-6	1098.7963	3e-8	|042)	5492.86	6.08	5492.91	6.00
|005)	1251.148	≤2e-6	1251.1525	1.8e-6	|034)	5717.85	5.245	5717.82	5.23
|111)	1386.880	1.05e-3	1386.8770	1.05e-3		5756	20.85	5752.56	21.13
|103)	1512.993	0.0128	1512.986	0.0126	|140)	5823.12	9.22	5823.02	9.29
|030)	1595.972	4e-6	1595.9708	3.2e-6	|026)	5846.5	62.6	5845.4	62.0
|201)	1633.526	0.0558	1633.518	0.0572		5872	49.8	5872.7	48.5
|022)	1897.242	7.5e-4	1897.247	7.60e-4	|230)	5976.83	45.9	5976.3	46.7
|300)	2069.6	29.5	2069.2	30.3	|132)	6049.7	36.2	6049.3	35.6
|014)	2105.537	0.741	2105.536	0.737		6201.9	42.1	6201.8	41.8
|006)	2208.16	0.0412	2208.198	0.0411	|051)	6209.04	2.079	6209.07	2.12
|120)	2223.85	3.265	2223.83	3.274				6299.7	104.2
|202)	2352.47	5.75	2352.38	5.77	|320)	6343.3	31.4	6343.9	31.2
|112)	2460.12	2.28	2460.11	2.32	|222)	6402.7	82.01	6402.3	81.7
|210)	2550.78	10.54	2550.71	10.63	|043)	6507.64	3.09	6507.59	3.10
|104)	2604.30	15.7	2604.40	15.93	|019)	6650.3	26.32	6652.99	26.96
|031)	2660.63	0.09753	2660.640	0.0981	|035)	6680	38.6	6679.8	37.9
|023)	2923.556	0.1881	2923.554	0.1888				6717.6	106.8
|015)	3077.5	5.04	3077.53	5.03	|027)	6759.11	35	6759.6	34.8
|007)	3132.82	0.8077	3132.991	0.814	|141)	6867.6	34	6867.6	33.5
|121)	3232.32	7.3	3232.327	7.31	|060)	6899.15	0.6	6899.107	0.594
|203)	3251.1	68.6	3251.3	67.5	|223)	6987	85.8	6986.8	85.7
|040)	3388.21	0.0786	3388.200	0.0782	|125)	7124.2	71.7	7124.2	71.7
|113)	3409.6	17.17	3409.66	17.18	|052)	7233.1	18.2	7233.23	18.26
|211)	3512.31	22.43	3512.29	22.39		7281	74	7281.1	74.1
|105)	3566.1	57.8	3565.6	57.9	|044)	7493.83	8.73	7493.84	8.68
|032)	3704.872	0.238	3704.866	0.240		7568	50.3	7563.4	52.2
|024)	3921.77	4.677	3921.77	4.687		7585.8	74.8	7587.2	68.6
|130)	3999.9	18.9	3999.84	19.80	|150)	7602.67	7.31	7602.63	7.29
			3999.2	32.8	|036)	7656.7	29.56	7656.64	29.68
|016)	4036.49	10.03	4036.63	9.94	|142)	7813.3	47	7813.1	48.1
|220)	4084.6	19.5	4084.71	20.25	|240)	7884.9	66.6	7884.9	66.2
|122)	4214.7	23.4	4214.49	23.12	|061)	7952.3	5.53	7952.29	5.52
|114)	4345.8	23.68	4345.79	23.80				8030.7	74.3
			4392.1	113.4	|224)	8171.1	105	8170.6	105.1
|041)	4436.7	9.9	4436.61	10.03	|151)	8232	30.3	8233.06	29.48
	4463.8	12.45	4463.70	12.44	|053)	8237.3	94	8236.6	96.1
|212)	4514.2	47.65	4514.1	47.8		8287.1	68.2	8287.2	66.9
|033)	4726.773	0.728	4725.768	0.727	|045)	8445.08	37.92	8444.9	37.9
|017)	4885.6	10.4	4885.78	9.98		8488	41	8486.7	37.5
			4887.8	65.6		8556.2	53	8557.5	52.6
			4938.4	112.9	|151)	8558	38	8557.7	39.0
|131)	5057.9	17	5057.81	17.12	|070)	8616.5	0.728	8616.421	0.717
|213)	5143.5	73.2	5143.6	73.5	|241)	8684	77	8687.8	76.3
|050)	5156.2	0.054	5155.939	0.0544	|143)	8802.3	90	8801.8	88.6
|123)	5275.7	32.1	5275.8	32.3		8921.4	90.9	8921.4	90.9
|221)	5400.2	46.8	5400.5	46.6	|062)	8973.7	7.7	8973.27	8.28
			5460.9	114.4					

Acknowledgments

We are grateful to Isabella Baccarelli for careful reading of the manuscript and Hua Guo, Bill Poirier and Tucker Carrington for useful discussions. We also thank Reinhard Schinke for sending us the HCO potential. V.A.M. acknowledges the NSF support, grant CHE-0108823. V.A.M. is Alfred P. Sloan research fellow.

References

1. V.A. Mandelshtam and H.S. Taylor, *J. Chem. Phys.* **103**, 2903 (1995).
2. V.A. Mandelshtam and H.S. Taylor, *J. Chem. Phys.* **107**, 6756 (1997).
3. V.A. Mandelshtam, *J. Chem. Phys.* **108**, 9999 (1998).
4. G. Li and H. Guo, *Chem. Phys. Lett.* **336**, 143 (2001).
5. G. Li and H. Guo, *Chem. Phys. Lett.* **347**, 443 (2001).
6. A. Neumaier and V. A. Mandelshtam, *Phys. Rev. Lett.* **86**, 5031-5034 (2001).
7. A.J.F. Siegert, *Phys. Rev.* **56**, 750 (1939).
8. G. Jolicard and E.J. Austin, *Chem. Phys. Lett.* **121**, 106 (1985).
9. D. Neuhauser and M. Baer, *J. Chem. Phys.* **91**, 4651 (1989).
10. T. Seideman and W.H. Miller, *J. Chem. Phys.* **96**, 4412 (1992).
11. U.V. Riss and H.-D. Meyer, *J. Phys. B*: *At. Mol. Opt. Phys.* **26**, 4503 (1993).
12. D.J. Tannor and D.E. Weeks, *J. Chem. Phys.* **98**, 3884 (1993).
13. D.J. Kouri, Y. Huang, W. Zhu and D.K. Hoffman, *J. Chem. Phys.* **100**, 3662 (1994).
14. S.-W. Huang and T. Carrington, Jr., *J. Chem. Phys.* **112**, 8765 (2000); B. Poirier and T. Carrington, Jr., *J. Chem. Phys.* **114**, 9254 (2001); S.-W. Huang and T. Carrington, Jr., *J. Chem. Phys.* **114**, 6485 (2001).
15. E.J. Heller, *J. Chem. Phys.* **68**, 3891 (1978).
16. G.G. Balint-Kurti, R.N. Dixon and C.C. Marston, *Faraday Trans. Chem. Soc.* **86**, 1741 (1990); J.Q. Dai and J.Z.H. Zhang, *J. Phys. Chem.* **100**, 6898 (1996).
17. M. R. Wall and D. Neuhauser, *J. Chem. Phys.* **102**, 8011 (1995).
18. V. A. Mandelshtam, *J. Phys. Chem* **105**, 2764-2769 (2001).
19. G.S. Armstrong and V.A. Mandelshtam, *J. Magn. Reson.* **153**, 22–31 (2001).
20. J. A. Fleck, J. R. Morris, Jr. and M. D. Feit, *Appl. Phys.* **10**, 129 (1976).
21. V.A. Mandelshtam and H.S. Taylor, *J. Chem. Phys.* **102**, 7390–7399 (1995)
22. R. Chen and H. Guo, *Comp. Phys. Comm.* **119**, 19 (1999).
23. S.K. Gray and G.G. Balint-Kurti, *J. Chem. Phys.* **108**, 950 (1998).
24. D.T. Colbert and W.H. Miller, *J. Chem. Phys.* **96**, 1982 (1992).
25. D.O. Harris, G.G. Engerholm and W.D. Gwinn, *J. Chem. Phys.* **43**, 1515 (1965).
26. N. Moiseyev, S. Freiedland and P.R. Certain, *J. Chem. Phys.* **74**, 4739 (1981).
27. B. Poirier and T. Carrington, Jr., *J. Chem. Phys.* **116**, 1215 (2002).
28. T.P. Grozdanov, V.A. Mandelshtam and H.S. Taylor, *J. Chem. Phys.* **103**, 7990 (1995).
29. H.-M. Keller, H. Floethmann, A.J. Dobbyn, R. Schinke, H.-J. Werner, C. Bauer and P. Rosmus, *J. Chem. Phys.* **105**, 4983 (1996).
30. Both double and quadruple precision versions of the FDM code, fdm.f, are available upon request. E-mail: mandelsh@uci.edu.
31. J.C. Light, I.P. Hamilton and J.V. Lill, *J. Chem. Phys.* **82**, 1400 (1985).
32. V. A. Mandelshtam and T. Carrington, Jr., *Phys. Rev.* **E65**, 028701 (2002).